


Fabrication and Evaluation of a pH-Responsive Nanocomposite-Based Colonic Delivery System for Improving the Oral Efficacy of Liraglutide

Jae Geun Song*, Da Hyun Kim*, Hyo-Kyung Han 

BK21 FOUR Team and Integrated Research Institute for Drug Development, College of Pharmacy, Dongguk University-Seoul, Goyang, 10326, Korea

*These authors contributed equally to this work

Correspondence: Hyo-Kyung Han, BK21 FOUR Team, College of Pharmacy, Dongguk University-Seoul, Dongguk-ro-32, Ilsan-Donggu, Goyang, 10326, Korea, Tel +82-31-961-5217, Fax +82-31-961-5206, Email hkhan@dongguk.edu

Purpose: Oral administration of liraglutide, a protein drug, suffers from low intestinal absorption and instability in the gastrointestinal tract, resulting in low bioavailability. The present study aimed to develop a pH-responsive nanocomposite based-colonic delivery system to improve the oral efficacy of liraglutide.

Methods: Nanocomplex (AC-Lira) between aminoclay and liraglutide was prepared by a spontaneous self-assembly. After surface charge reversal using citric acid, AC-Lira was coated with poly(methacrylic acid-co-methyl methacrylate) (1:2). The fabricated nanocomplex underwent various in vitro studies to characterize its physicochemical properties, drug release, and cellular transport. In vivo efficacy studies were also conducted using streptozotocin-induced diabetic rats.

Results: Both uncoated (AC-Lira) and coated nanocomplex (EAC-Lira) achieved high entrapment efficiency (> 90%) and showed a narrow size distribution. While exhibiting low drug release at pH 1.2 (approximately 30%), EAC-Lira achieved rapid and extensive drug release (~90%) at pH 7.4, displaying pH-dependent drug release. EAC-Lira showed significant size reduction and surface charge reversal during dissolution at pH 7.4, probably due to the removal of the outer coating layer. Furthermore, EAC-Lira was effective at protecting the entrapped proteins against enzymatic degradation. EAC-Lira also increased the membrane transport of liraglutide by 3.5 folds in Caco-2 cells. Owing to enhanced membrane transport and metabolic stability, EAC-Lira improved in vivo efficacy of orally administered liraglutide, significantly reducing blood glucose concentrations, intake of food and water, and body weight in type 2 diabetes rats.

Conclusion: These results suggest EAC-Lira is a promising approach to improving the oral bioavailability and efficacy of liraglutide.

Keywords: liraglutide, aminoclay, GLP-1 agonist, type 2 diabetes, nanocomposite

Introduction

High potency, selectivity, and low toxicity of protein drugs increase their desirability for treating various incurable and chronic diseases.^{1,2} However, low metabolic stability and poor membrane permeability of therapeutic proteins result in low bioavailability; hence, most protein drugs are available in injectable formulations in the current pharmaceutical market. Therefore, patient-friendly oral formulations of protein drugs are necessary to improve patient compliance, particularly in long-term therapy for chronic diseases.

Diabetes is one of the most common chronic diseases globally.³ In 2021, the number of patients with diabetes was estimated at 537 million; it is expected to reach 783 million by 2045.⁴ Specially, type 2 diabetes is prevalent in 90% of diabetes patients and is a leading cause of mortality, increasing the risk of various diseases, including cardiovascular disorders, blindness, renal failure, and chronic liver diseases.^{4,5} For more effective treatment of type 2 diabetes, protein drugs are often used as anti-diabetic medications, besides traditional synthetic small molecules. For example, liraglutide is a long-acting, fatty acylated glucagon-like peptide-1 (GLP-1) analog, which shares 97% homology to human GLP-1 except

for two parts: arginine residue at position 34 instead of lysine and a fatty acid side chain (C_{16} , palmitic acid) attached to the lysine at position 26 via glutamate spacer.^{6–8} Liraglutide is used for type 2 diabetes, obesity, and chronic weight management.⁹ Compared to insulin therapy, liraglutide has the following advantages:^{10,11} (i) minimizing the risk of hypoglycemia, (ii) a long half-life of approximately 13 h, (iii) inhibiting gastric emptying and reducing appetite and food intake. In current medical practice, liraglutide is administered once daily by subcutaneous injection. Given that oral delivery is a highly desirable alternative to injections, particularly in chronic diseases requiring repeated dosing for prolonged periods, this study aimed to develop a pH-responsive nanocomposite system for effective oral delivery of liraglutide.

Aminoclay is a 3-aminopropyl-functionalized magnesium phyllosilicate. It is dispersed in water as cationic nano-sheets.¹² It provides several advantages; (i) it can produce a nanocomplex with a diverse range of drugs via electrostatic interactions, and (ii) it has low risk of toxicity, enhancing cellular drug uptake.^{13,14} It can also improve the thermal stability of protein drugs.¹⁵ Therefore, in this study, an aminoclay-based colonic nanocomposite system was fabricated as an oral delivery system of liraglutide as illustrated in Figure 1. First, the core nanocomplex between aminoclay and liraglutide was fabricated via a spontaneous co-assembly, and then, the surface charge of the nanocomplex was reversed to positive using citric acid. Finally, the core-nanocomplex underwent a surface coating with poly(methacrylic acid-co-methyl methacrylate) (1:2), a pH-dependent polymer.¹⁶ In this study, we developed a direct coating method between two repulsive components via a charge modification in acidic conditions, demonstrating a new manufacturing process of pH-dependent nanoparticles loaded with protein drugs.

Materials and Methods

Materials

Liraglutide was obtained from Chengdu Shengnuo Biopharm Co., Ltd. (Chengdu, China). Streptozotocin (STZ), 3-aminopropyltriethoxysilane (APTES, 99%), citric acid, pepsin, and trypsin were purchased from Sigma-Aldrich Co. (St Louis, MO, USA). Inorganic salts including magnesium chloride hexahydrate (98%) were obtained from Junsei Chemical Co., Ltd (Tokyo, Japan). Poly(methacrylic acid-co-methyl methacrylate) (1:2) (Eudragit® S100,

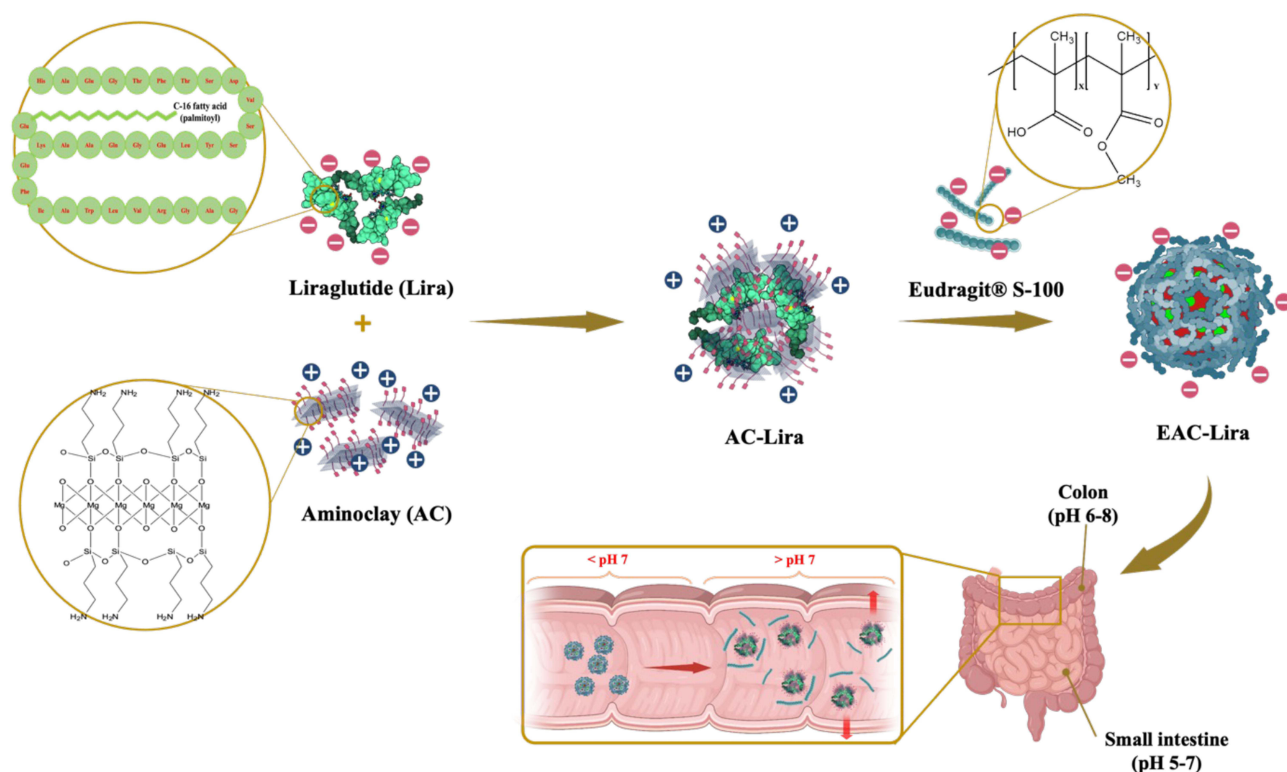


Figure 1 Fabrication of a pH-responsive nanocomposite-based colonic delivery system to improve the oral absorption of liraglutide.

ES100) was provided by Evonik Korea Ltd. (Seoul, Korea). 3-Aminopropyl functionalized magnesium phyllosilicate (aminoclay) was prepared as described in previous studies.¹⁷ Hank's balanced salt solution (HBSS), Dulbecco's Modified Eagle's medium (DMEM), fetal bovine serum (FBS), penicillin-streptomycin, and non-essential amino acids were purchased from GE Healthcare Life Sciences (South Logan, UT, USA).

Cells

Caco-2 cells were provided by the Korean Cell Line Bank (Seoul, Korea). Cells were grown in a DMEM medium with 10% FBS, 1% antibiotics, and 1% nonessential amino acid. Cells were incubated at 37 °C in an atmosphere of 5% CO₂ and 90% relative humidity.

Preparation of Nanoparticles

Liraglutide (10 mg/mL) was dissolved in distilled water and added dropwise into an aqueous solution of aminoclay (10 mg/mL) at a drug/clay ratio of 1:3 with stirring at 350 rpm. After stirring for 1 h, a white precipitate was collected by centrifugation (22,250×g) at 4 °C for 15 min and dried at room temperature under vacuum. The obtained nanoparticles (AC-Lira, 20 mg) were dispersed in 10 mM citric acid (1mL, pH 3) and added dropwise into 2% poly methacrylate copolymer (ES100) in organic solvent (ethanol: acetone = 1:2, v/v) at an AC-Lira/ ES100 ratio of 1:2 (v/v). After vigorous stirring for 30 min, the coated nanoparticles (EAC-Lira) were collected by centrifugation (22,250×g) at 4 °C for 15 min, and dried at room temperature under vacuum.

Structural Characterization

Particle size and zeta potential of all formulations were measured by dynamic light scattering (DLS) using a Zetasizer (Nano-ZS90; Malvern Instruments, Malvern, UK). The polydispersity index (PDI) was also estimated to examine the size distribution. The entrapment efficiency (EE) of the nanoparticles was calculated using the following equation:

$$EE (\%) = \frac{\text{Drug amount initially added} - \text{Drug amount in supernatant}}{\text{Drug amount initially added}} \times 100$$

The structural stability of liraglutide entrapped in the nanoparticles was examined by Circular dichroism (CD) analysis using the Chirascan™-Plus Spectrometer (Applied Photophysics, Surrey, UK). Spectra were obtained from 200 nm to 260 nm at 25 °C (a light path length: 5 mm, a bandwidth: 1 nm). Fourier-transform infrared spectroscopy (FT-IR) (Nicolet™ iS™ 5; Thermo Fisher Scientific Inc., Waltham, MA, USA) analysis was also performed with a ZnSe crystal accessory. FT-IR spectra of all samples were measured over a wavenumber range of 4000–500 cm⁻¹ with 64 scans at a resolution of 4 cm⁻¹. The morphological characteristics of nanoparticles were examined using a transmission electron microscope (TEM) (JEM-F200; JEOL Ltd., Tokyo, Japan) at the National Center for Inter-University Research Facilities (NCIRF) at Seoul National University (Seoul, Korea).

In vitro Drug Release Studies

The drug release studies of nanoparticles were performed at pH 1.2 and 7.4 to evaluate pH-dependent drug release characteristics. As release media, 0.1 M hydrochloride buffer and 0.05 M phosphate buffer were prepared and adjusted to pH 1.2 and 7.4, respectively. Each formulation (equivalent to 0.2 mg of liraglutide) was incubated in the release medium (3 mL) at 37 °C while shaking at 100 rpm. At the predetermined time points, the samples were withdrawn and centrifuged (22,250×g) for 10 min. Drug concentrations in supernatants were determined by an HPLC assay. Change in the particle size, zeta-potential, and PDI of nanoparticles during incubation in dissolution media were also evaluated using a Zetasizer (Nano-ZS90; Malvern Instruments, Malvern, UK).

Protection Against Enzymatic Degradation

The conformational stability of liraglutide entrapped in nanoparticles was investigated using simulated gastric fluid (SGF, pH 1.2 with 5 µg/mL pepsin) and intestinal fluid (SIF, pH 7.4 with 20 µg/mL trypsin), as reported previously with slight modification.¹⁸ The nanoparticles were incubated in SGF or SIF at 37 °C and the enzymatic reaction was terminated at the predetermined time points by adding 0.2 M NaOH (0.2 mL) into SGF and 0.1 M HCl (0.2 mL) into SIF. The nanoparticles were collected by centrifugation (22,250×g) for 15 min, and liraglutide in nanoparticles was extracted in PBS (pH 7.4) for 2 h. The secondary structure of liraglutide released from nanoparticles was examined by CD spectroscopy and compared to that of native liraglutide.

Transport Studies

Caco-2 cells were seeded on the trans-well plates (surface area of each well: 1.12 cm²) at a cell density of 2.0×10⁵ cells/well. Cells were incubated at 37 °C for 21 days, and the medium was changed every other day. During incubation, the integrity of cell monolayers was monitored regularly by determining trans-epithelial electrical resistance (TEER) values using an epithelial tissue voltohmmeter (Millicell ERS-2; MerckKGaA, Darmstadt, Germany). Prior to the transport studies, the medium was removed, and cells were washed twice with HBSS. Both apical and basolateral compartments were filled with HBSS and pre-incubated for 30 min at 37 °C. Then, HBSS in the apical side was replaced by a drug solution containing each formulation equivalent to 200 µg/mL of liraglutide. At predetermined time points, samples (150 µL) were collected from the basolateral side, and an equal volume of fresh HBSS was added to the basolateral side to maintain a constant volume. Drug concentrations were determined using an HPLC assay. The apparent permeability coefficient (P_{app}) was calculated as follows; $P_{app} = dQ/dt \times 1/AC_0$ (C_0 : the initial drug concentration in the apical compartment, A : the surface area of membrane filter, and dQ/dt : the cumulative drug amount as a function of time in the basolateral compartment).

TEER values were also monitored during the transport studies. After removing the drug solution at the end of transport studies, fresh HBSS was added into the apical and basolateral compartments, and TEER values were measured for 24 h.

Pharmacokinetics Studies

The pharmacokinetic characteristics of EAC-Lira were examined in rats and the experimental protocol was approved by the Review Committee of Dongguk University (IACUC-2022-009-1). Male Sprague-Dawley rats (230–250g) were provided by Orient Bio Inc. (Seongnam, Korea). Rats were divided into two groups ($n = 4$ per group) and administered orally liraglutide or EAC-Lira. Each formulation was dispersed in 0.5% aqueous methylcellulose and administered orally at a dose equivalent to 15 mg/kg of liraglutide. Blood samples were collected from the jugular vein at 0.5, 1, 2, 4, 6, 8, 12, 24 and 30 h after dosing. Blood samples were centrifuged at 16,600 × g for 10 min at 4 °C, and the separated plasma samples were stored at –80 °C until analyzed by LC-MS/MS.

In vivo Efficacy Studies

Animal studies were conducted in accordance with the “Guiding Principles in the Use of Animals in Toxicology” adopted by the Society of Toxicology (USA), and the study protocol was approved by the review committee of Dongguk University (IACUC-2022-009-1). Male Sprague-Dawley rats were provided by Orient Bio Inc. (Seongnam, Korea). As previously reported,¹⁷ all rats were fed a high-fat diet (HFD) for 3 weeks, and type 2 diabetes was induced with streptozotocin (STZ) (in 50 mM citrate buffer solution, pH 4.5) via intraperitoneal (IP) injection at 40 mg/kg. After 10 days, blood was collected from the jugular vein to determine blood glucose concentrations by a Roche glucose meter (ACCU-CHEK® guide). Rats with fasting blood glucose over 300 mg/dL were used as diabetic models.

The pharmacodynamics effects of liraglutide were evaluated in STZ-induced type 2 diabetic rats. Animals were divided into four groups ($n = 5$ –6/group). Group 1 was given a vehicle by SC injection. Group 2 was treated subcutaneously with liraglutide solution once daily at a dose of 300 µg/kg. Groups 3 and 4 were administered

liraglutide solution and EAC-Lira orally at a dose equivalent to 15 mg/kg of liraglutide. Changes in blood glucose concentrations, intake of food and water, and body weight were examined for 30 days. Each day, the rats were given a predetermined amount of HFD and normal tap water;¹⁸ after 24 h, the quantity of remaining food and water was measured. The body weight of each diabetic rat was measured daily using a micro-weighing balance. Blood samples were collected from the jugular vein under aseptic conditions, and blood glucose concentrations were determined using a Roche glucose meter (ACCU-CHEK guide). All physiological parameters were expressed as a percentage of initial levels on Day 0 before the drug administration.

Analytical Method

In vitro Samples

Drug concentrations were determined using an HPLC system (Ultimate 3000 HPLC; Thermo fisher, Waltham, MA, USA) and a reversed-phase column (Gemini[®] C18, 4.6×150 mm, 5 µm; Phenomenex, Torrance, CA, USA). The mobile phase consisted of (A) 0.1% trifluoroacetic acid (TFA) in acetonitrile and (B) 0.1% trifluoroacetic acid (TFA) in water. The flow rate was 0.6 mL/min and the column temperature was 40 °C. The analytes were separated using a linear gradient changing from 60% B to 50% B within 2.5 min and then to 40% B for 0.5 min, which was maintained for 1 min. Mobile phase B was changed from 40% to 50% over 2 min and then to 60% B for 1 min, which was maintained for 3 min. The detection wavelength was 220 nm, and tolbutamide was used as an internal standard. The calibration curve was linear over the drug concentration of 1–200 µg/mL, displaying good linearity ($r^2 > 0.998$).

In vivo Samples

Drug concentrations in plasma were measured using LC-MS/MS assay. Mobile phases (A: 0.1% formic acid in water, B: 0.1% formic acid in acetonitrile) were eluted through a C18 column (2.1×50 mm, 5.0 µm; Phenomenex, CA, USA) at 40 °C with the flow rate of 0.25 mL/min. The analytes were separated using a linear gradient changing from 30% B to 60% B within 0.5 min and then to 90% B for 0.5 min, which was maintained for 1.5 min. Mobile phase B was then changed from 90% to 30% over 0.1 min and maintained for 2.4 min. An API 4000 triple quadrupole mass spectrometer (ABSciex, Framingham, MA, USA) with an electrospray ionization (ESI) source was used for mass analysis. The precursor/product ion pair (m/z) for Lira was 938.8/1128.3 and the calibration curve was linear ($r^2 > 0.999$) over the concentration range of 5–1000 ng/mL.

Statistical Analysis

All mean values are expressed with their standard deviation (mean ± SD). Statistical significance was determined using a Student's *t*-test or one-way ANOVA. A *p*-value less than 0.05 indicated statistically significant difference.

Results and Discussion

Preparation and Structural Characterization of Nanoparticles

As summarized in Table 1, all nanoparticles exhibited high entrapment efficiency (> 90%) and narrow size distribution. First, the liraglutide-aminoclay nanocomplex (AC-Lira) was prepared via spontaneous self-assembly, where positively charged aminoclay could effectively interact with negatively charged liraglutide. The obtained nanoparticles (AC-Lira) had an average size of 146 ± 20.6 nm and a zeta-potential of -29.8 ± 2.08 mV (Table 1). Subsequently, when AC-Lira was dispersed into 10 mM citric acid (pH 3), its surface charge reversed to positive since liraglutide has an isoelectric point of 4.9.¹⁹ Therefore, it could undergo direct surface coating with anionic polymethacrylate copolymers, thus producing a colonic delivery system of liraglutide (EAC-Lira). In previous studies, the negatively charged nanocomplex

Table 1 Characteristics of Nanoparticles (Mean ± SD, n = 3)

Formulation	Size (nm)	PDI	Zeta Potential (mV)	EE (%)
AC-Lira	145.7 ± 20.6	0.226 ± 0.07	-29.8 ± 2.08	99.7 ± 0.07
EAC-Lira	370.4 ± 13.9	0.163 ± 0.05	-1.97 ± 0.09	90.7 ± 0.09

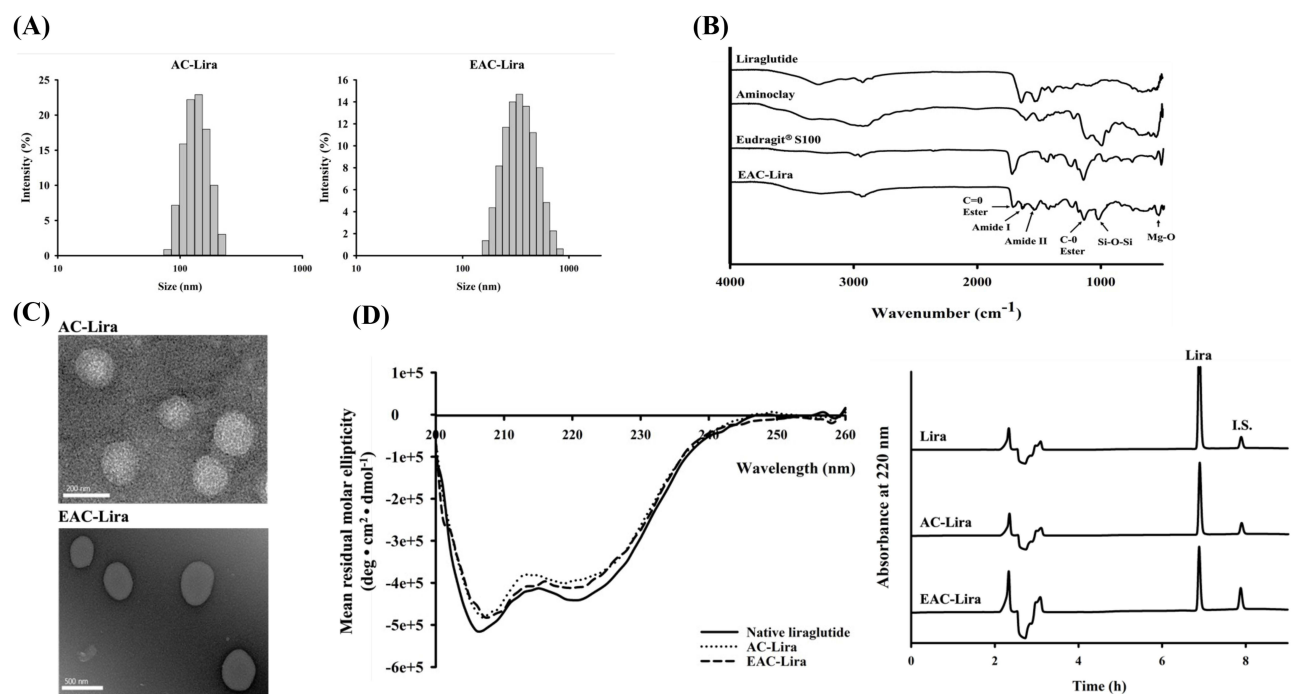


Figure 2 In vitro characterization of aminoclay-based nanoparticles. **(A)** Size distribution of nanoparticles, **(B)** FT-IR spectra, **(C)** TEM images. Scale bar is 200 nm for AC-Lira and 500 nm for EAC-Lira, **(D)** CD spectra (left) and HPLC chromatograms (right) of liraglutide released from each formulation after incubation at pH 7.4 for 8 h. **Abbreviation:** I.S., internal standard.

underwent a dual coating process via layer-by-layer deposition to fabricate pH-responsive drug delivery systems when the enteric coating polymers had the same surface charge as the nanocomplex.^{20–22} However, in this study, the modulation of surface charges using citric acid allowed a direct coating between two repulsive components, simplifying the manufacturing process of pH-dependent nanoparticles. EAC-Lira was obtained with an average size of 370 ± 13.9 nm in a narrow size distribution (Table 1 and Figure 2A).

Structural and morphological characteristics of nanoparticles were examined using a CD analysis, FT-IR, and TEM. As summarized in Figure 2B, the FT-IR spectrum of EAC-Lira exhibited absorption bands from each formulation component, including peaks at 1652 cm^{-1} (amide I peak) and 1541 cm^{-1} (amide II peak) from liraglutide, peaks at 1009 cm^{-1} (Si–O–Si) and 550 cm^{-1} (Mg–O) from aminoclay, and absorption bands at 1723 cm^{-1} (C=O ester) and 1146 cm^{-1} (C–O ester) from polymethacrylate copolymer (ES100). This result suggests the formation of a liraglutide-aminoclay complex. Moreover, the morphology of nanoparticles was examined using TEM. All nanoparticles were spherical and their size was correlative to that measured by dynamic light scattering (Figure 2C). Given that the conformational stability is critical in formulating proteins, the secondary structure of liraglutide entrapped in nanoparticles was examined by CD spectroscopy. As shown in Figure 2D, the CD spectra of liraglutide released from nanoparticles were similar to that of native liraglutide, implying that nanoparticles maintained conformational stability of liraglutide. Furthermore, HPLC analysis confirmed the intact drug peak without any significant degradation products when the entrapped liraglutide was released from nanoparticles (Figure 2D).

Collectively, liraglutide-loaded nanoparticles with/without surface coating were obtained in a spherical shape with high entrapment efficiency ($> 90\%$) and effectively maintained the structural stability of the entrapped protein.

In vitro Drug Release Studies

Drug release studies were performed at pH 1.2 and 7.4 to confirm a pH-dependent drug release of nanoparticles. As shown in Figure 3A, AC-Lira exhibited rapid drug release at acidic pH, releasing about 80% of the drugs within 30 min. In contrast, the coated nanoparticles (EAC-Lira) showed drug release of less than 30% at pH 1.2, achieving rapid and extensive drug release at pH 7.4 with approximately 90% over 12 h (Figure 3B). The pH-dependent drug release of EAC-

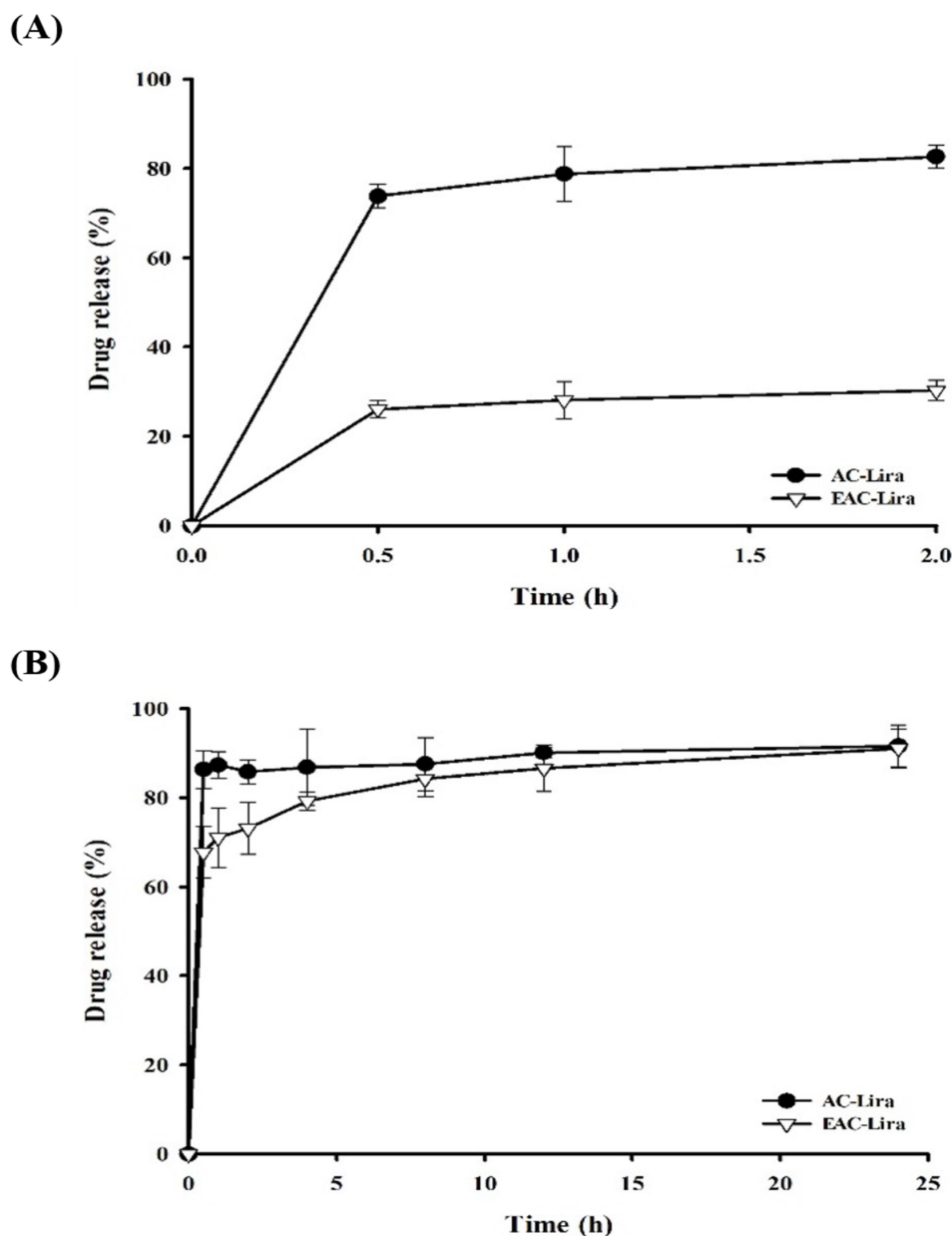


Figure 3 In vitro drug release profiles of the uncoated (AC-Lira) and coated (EAC-Lira) nanoparticles at pH 1.2 (A) and at pH 7.4 (B) (mean \pm SD, n = 3).

Lira could be due to peeling of the polymer coating layer at pH above 7.0. This is also supported by the changes in the size and surface charge of nanoparticles as shown in Figure 4. While particle size and zeta potential of EAC-Lira were maintained under incubation at pH 1.2, the particle size significantly reduced with the alteration in surface charge under incubation at pH 7.4. The pH-dependent drug release characteristics of EAC-Lira may prevent drug release in the harsh environment of the stomach and deliver more drugs into intestinal sites.

Protection Against Enzymatic Degradation

Proteolytic enzymes in the gastrointestinal (GI) tract can cause the destabilization of protein drugs, leading to low oral bioavailability. The protective effect of nanoparticles against enzymatic degradation of liraglutide in the GI tract was examined using simulated gastric fluid (SGF) and intestinal fluid (SIF) containing digestive enzymes.^{23,24} As shown in Figure 5A, liraglutide entrapped in AC-Lira was destabilized in SGF. In contrast, the secondary structure of liraglutide

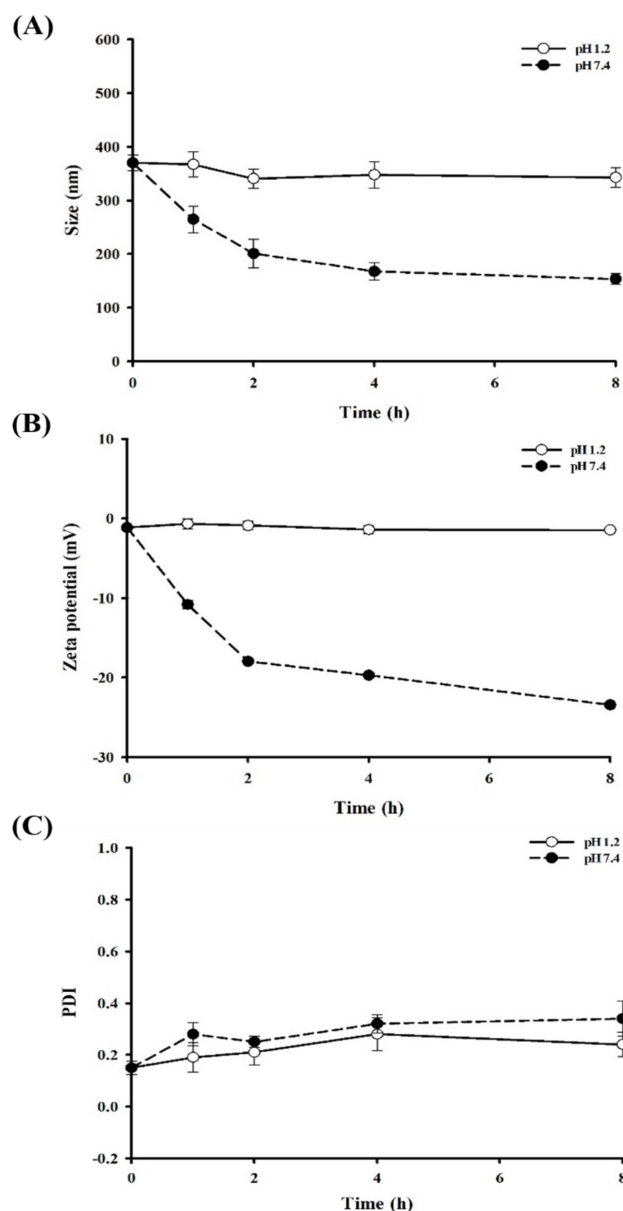


Figure 4 Variation in particle size (A), zeta potential (B), and PDI (C) during the incubation of EAC-Lira at different pH values (mean \pm SD, $n = 3$).

entrapped in EAC-Lira was similar to that of native liraglutide in both SGF and SIF (Figure 5A and B). These results were also consistent with the observation from the HPLC analysis of liraglutide released from nanoparticles. As shown in Figure S1, HPLC chromatograms from EAC-Lira indicated the intact drug peak without any additional impurities in the presence of digestive enzymes. These results suggest that EAC-Lira could successfully protect the proteins against enzymatic degradation during the transition in the GI tract.

Cellular Transport

Effect of nanoparticles on the cellular uptake of liraglutide was examined in Caco-2 cells. As shown in Figure 6A, all nanoparticles increased drug transport by 3.5–3.8 folds in Caco-2 cells compared to free drug. It may be attributed, at least in part, to the transient tight junction (TJ) opening in the presence of nanoparticles. As shown in Figure 6B, TEER values significantly decreased on cell exposure to AC-Lira and EAC-Lira, but fully recovered when nanoparticles were removed at

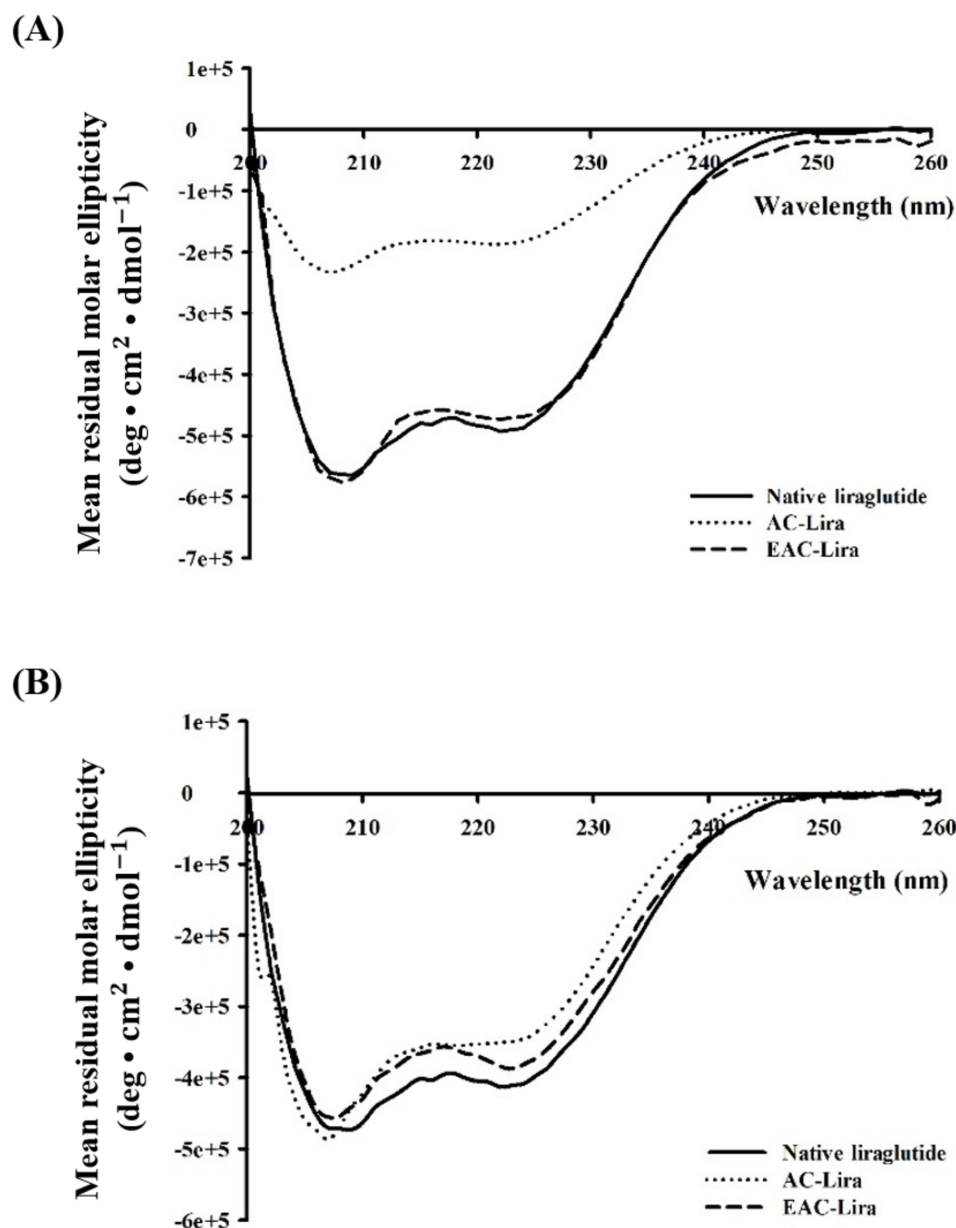


Figure 5 CD spectra of liraglutide released from the nanoparticles after incubation in SGF (A) and SIF (B). At the end of incubation in SGF and SIF, the nanoparticles were collected and incubated in PBS (pH 7.4). The released liraglutide underwent CD spectroscopic analysis.

the end of the experiment. EAC-Lira was converted to AC-Lira after the dissolution of outer coating layer at pH 7.4 and thus, both EAC-Lira and AC-Lira showed similar TJ opening effect during the incubation in Caco-2 cells (Figure 6B). The transient TJ opening effect of these nanoparticles may be explained, at least in part, as follows. First, as shown in Figure 3B, AC-Lira released drugs rapidly at pH 7.4 (greater than 80% drug release within 0.5 h). During this drug release process, the dissociation of nanocomplex also released the positively charged free aminoclay, a transient TJ opener.^{14,25} The effect of cationic aminoclay on the reversible TJ opening has been clearly demonstrated in the previous studies.^{14,25} Second, the protonated amine groups of aminoclay outward from the surface of AC-Lira (ie, outward-facing of nanocomplex) were not occupied by liraglutide, which might interact with negatively charged cell membrane and TJ components. Although the exact mechanism of TJ opening remains unknown, the result suggests that aminoclay-based nanoparticles have a transient and reversible effect on TJ opening and facilitate drug permeation via paracellular pathway.²⁶

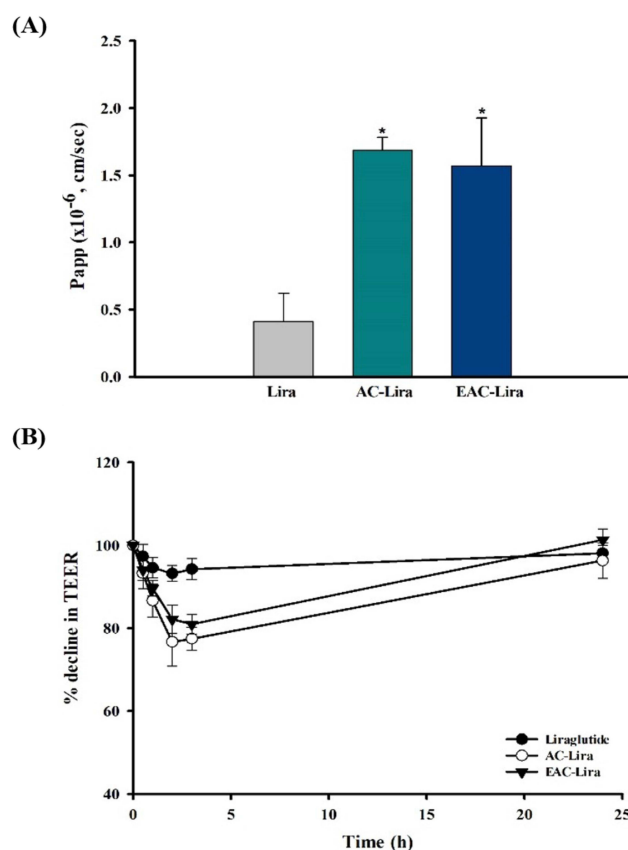


Figure 6 Cellular transport of liraglutide in different formulations (mean \pm SD, $n = 4$). **(A)** Apparent permeability of liraglutide from different formulations, and **(B)** the effect of each formulation on the trans-epithelial electrical resistance (TEER). * $p < 0.05$, compared to the control (liraglutide solution).

In vivo Efficacy Studies

The in vivo effectiveness of EAC-Lira as an oral delivery system was evaluated in type 2 diabetic rats. In vivo efficacy of EAC-Lira in alleviating the symptoms of diabetes and obesity was examined in comparison with SC injection. Given that glucagon-like peptide-1 receptor agonists such as liraglutide stimulate insulin secretion and decrease food and water intake by delaying gastric emptying,¹¹ the in vivo efficacy of each formulation was evaluated based on the change in blood glucose level, food/water intake, and body weight. As shown in Figure 7A, SC injection of free drug solution significantly reduced blood glucose concentrations, achieving approximately 70% of the initial blood glucose level on day 7. However, oral administration of free drug solution did not show any hypoglycemic effect, probably due to gastrointestinal destabilization and poor membrane permeability. In contrast, oral administration of EAC-Lira gradually reduced blood glucose concentrations, reaching approximately 80% of the initial blood glucose level on day 10. These results are consistent with the observation from pharmacokinetics studies (Table S1 and Figure S2). As shown in Figure S2, the systemic exposure of liraglutide was not detectible after the oral administration of pure drug solution. In contrast, EAC-Lira significantly improved the oral exposure of liraglutide, where the C_{max} and AUC of liraglutide were 71.1 ± 36.3 ng/mL and 480 ± 253 ng•h/mL, respectively.

In addition to the modulation of blood glucose levels, the study examined the efficacy of EAC-Lira against obesity in diabetic rats. Like SC injection, once-daily dosing of EAC-Lira significantly reduced food intake by 40–50% and water consumption by 50–60% compared to the control group (Figure 7B and C). Accordingly, EAC-Lira showed a significant effect in weight loss, steadily reducing body weight over 30 days (Figure 7D). These results suggest a high potential of EAC-Lira as an effective oral delivery system of liraglutide, improving the symptoms in diabetes and obesity.

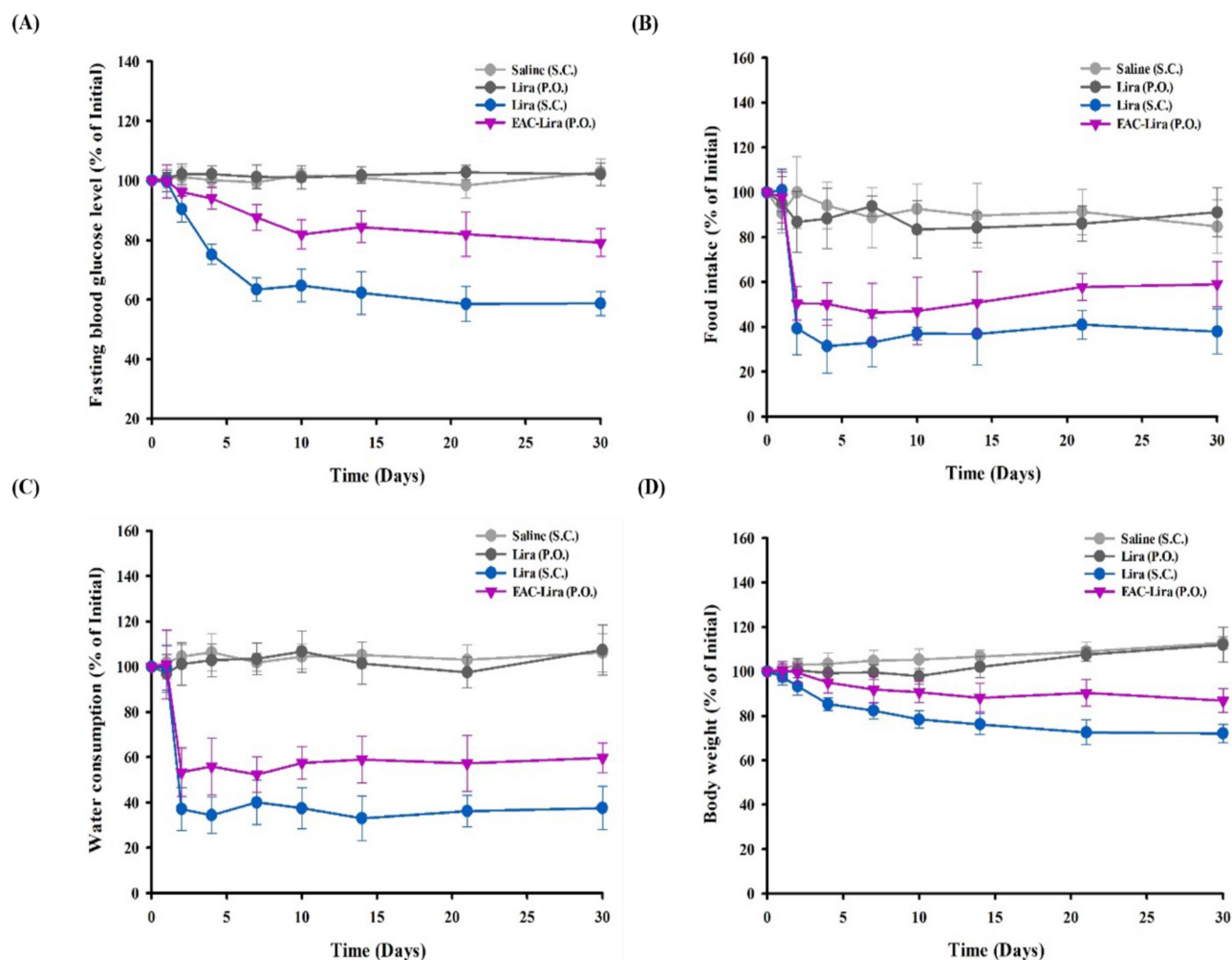


Figure 7 In vivo efficacy of EAC-Lira in type 2 diabetic rats (mean \pm SD, $n = 5-6$). The in vivo effect on blood glucose level (A), food intake (B), water consumption (C), and body weight (D) was assessed after once-daily dosing of each formulation for 30 days. The dose was equivalent to 0.3 mg/kg and 15 mg/kg of liraglutide, for SC injection and oral administration, respectively.

Conclusions

In this study, EAC-Lira was developed for improved oral bioavailability of liraglutide. EAC-Lira was obtained as a nano-sized particle, displaying narrow size distribution and high entrapment efficiency ($> 90\%$). It showed pH-dependent drug release characteristics, minimizing premature drug release in the upper GI tract. EAC-Lira could retain the structural stability of entrapped proteins in the presence of digestive enzymes. Furthermore, EAC-Lira significantly improved cellular drug uptake. Thus, orally administered EAC-Lira could reduce blood glucose levels, intake of food and water, and body weights in type 2 diabetic rats. Taken together, EAC-Lira may be a promising oral delivery system of liraglutide.

Data Sharing Statement

All data generated or analyzed during this study are included in this published article.

Ethics Approval and Informed Consent

All animal studies were approved by the review committee of Dongguk University (IACUC-2022-009-1).

Funding

This research was supported by National Research Foundation of Korea (NRF) grant funded by the Korea government (MSIT) (Nos. 2019R1A2C2004873 and 2018R1A5A2023127) and the BK21 FOUR program through the National Research Foundation (NRF) funded by the Ministry of Education of Korea.

Disclosure

The authors declare that they have no competing interests.

References

1. Lagassé HD, Alexaki A, Simhadri VL, et al. Recent advances in (therapeutic protein) drug development. *F1000Research*. 2017;6:113.
2. Bajracharya R, Song JG, Back SY, Han H-K. Recent advancements in non-invasive formulations for protein drug delivery. *Comput Struct Biotechnol J*. 2019;17:1290–1308.
3. Caughey GE, Vitry AI, Gilbert AL, Roughead EE. Prevalence of comorbidity of chronic diseases in Australia. *BMC Public Health*. 2008;8:1–13.
4. Sun H, Saeedi P, Karuranga S, et al. IDF Diabetes Atlas: global, regional and country-level diabetes prevalence estimates for 2021 and projections for 2045. *Diabetes Res Clin Pract*. 2022;183:109119.
5. Jacobsen LV, Flint A, Olsen AK, Ingwersen SH. Liraglutide in type 2 diabetes mellitus: clinical pharmacokinetics and pharmacodynamics. *Clin Pharmacokinet*. 2016;55:657–672.
6. Vilsbøll T. Liraglutide: a once-daily GLP-1 analogue for the treatment of type 2 diabetes mellitus. *Expert Opin Investig Drugs*. 2007;16(2):231–237.
7. Wajsborg E, Amarah A. Liraglutide in the management of type 2 diabetes. *Drug Des Devel Ther*. 2010;279–290.
8. Sharma AN, Ligade SS, Sharma JN, Shukla P, Elased KM, Lucot JB. GLP-1 receptor agonist liraglutide reverses long-term atypical antipsychotic treatment associated behavioral depression and metabolic abnormalities in rats. *Metab Brain Dis*. 2015;30:519–527.
9. Lin C-H, Shao L, Zhang Y-M, et al. An evaluation of liraglutide including its efficacy and safety for the treatment of obesity. *Expert Opin Pharmacother*. 2020;21(3):275–285.
10. Drucker DJ. Advances in oral peptide therapeutics. *Nat Rev Drug Discov*. 2020;19(4):277–289.
11. Ismail R, Csoka I. Novel strategies in the oral delivery of antidiabetic peptide drugs—Insulin, GLP 1 and its analogs. *Eur J Pharm Biopharm*. 2017;115:257–267.
12. Patil AJ, Mann S. Self-assembly of bio-inorganic nanohybrids using organoclay building blocks. *J Mater Chem*. 2008;18(39):4605–4615.
13. Lee SH, Back S-Y, Song JG, Han H-K. Enhanced oral delivery of insulin via the colon-targeted nanocomposite system of organoclay/glycol chitosan/Eudragit® S100. *J Nanobiotechnology*. 2020;18(1):1–10.
14. Lee SH, Song JG, Han H-K. Development of pH-responsive organic-inorganic hybrid nanocomposites as an effective oral delivery system of protein drugs. *J Control Release*. 2019;311:74–84.
15. Song JG, Lee SH, Han H-K. Biophysical evaluation of aminoclay as an effective protectant for protein stabilization during freeze-drying and storage. *Int J Nanomed*. 2016;11:6609.
16. Xiao B, Si X, Zhang M, Merlin D. Oral administration of pH-sensitive curcumin-loaded microparticles for ulcerative colitis therapy. *Colloids Surf B*. 2015;135:379–385.
17. Furman BL. Streptozotocin-induced diabetic models in mice and rats. *Curr Protoc Pharmacol*. 2015;70(1):5.47. 1–5.47. 20.
18. Senduran N, Yadav HN, Vishwakarma VK, et al. Orally deliverable nanoformulation of liraglutide against type 2 diabetic rat model. *J Drug Deliv Sci Technol*. 2020;56:101513.
19. Presas E, Tovar S, Cuñarro J, O'Shea JP, O'Driscoll CM. Pre-clinical evaluation of a modified cyclodextrin-based nanoparticle for intestinal delivery of liraglutide. *J Pharm Sci*. 2021;110(1):292–300.
20. Song JG, Lee SH, Han H-K. Development of an M cell targeted nanocomposite system for effective oral protein delivery: preparation, in vitro and in vivo characterization. *J Nanobiotechnology*. 2021;19:1–11.
21. M-G L, W-L L, Wang J-C, et al. Preparation and characterization of insulin nanoparticles employing chitosan and poly (methylmethacrylate/methylmethacrylic acid) copolymer. *J Nanosci Nanotechnol*. 2006;6(9–10):2874–2886.
22. Zhao M, Lee SH, Song JG, Kim HY, Han H-K. Enhanced oral absorption of sorafenib via the layer-by-layer deposition of a pH-sensitive polymer and glycol chitosan on the liposome. *Int J Pharm*. 2018;544(1):14–20.
23. Dubey SK, Parab S, Dabholkar N, et al. Oral peptide delivery: challenges and the way ahead. *Drug Discov Today Technol*. 2021;26(4):931–950.
24. Peppas NA, Kavimandan NJ. Nanoscale analysis of protein and peptide absorption: insulin absorption using complexation and pH-sensitive hydrogels as delivery vehicles. *Eur J Pharm Sci*. 2006;29(3–4):183–197.
25. Kim S-Y, Kwon W-A, Shin S-P, et al. Electrostatic interaction of tumor-targeting adenoviruses with aminoclay acquires enhanced infectivity to tumor cells inside the bladder and has better cytotoxic activity. *Drug Deliv*. 2018;25(1):49–58.
26. Azevedo C, Macedo MH, Sarmento B. Strategies for the enhanced intracellular delivery of nanomaterials. *Drug Discov Today*. 2018;23(5):944–959.

International Journal of Nanomedicine

Dovepress

Publish your work in this journal

The International Journal of Nanomedicine is an international, peer-reviewed journal focusing on the application of nanotechnology in diagnostics, therapeutics, and drug delivery systems throughout the biomedical field. This journal is indexed on PubMed Central, MedLine, CAS, SciSearch®, Current Contents®/Clinical Medicine, Journal Citation Reports/Science Edition, EMBase, Scopus and the Elsevier Bibliographic databases. The manuscript management system is completely online and includes a very quick and fair peer-review system, which is all easy to use. Visit <http://www.dovepress.com/testimonials.php> to read real quotes from published authors.

Submit your manuscript here: <https://www.dovepress.com/international-journal-of-nanomedicine-journal>